Energies **2012**, *5*, 5363-5371; doi:10.3390/en5125363

OPEN ACCESS

energies

ISSN 1996-1073

www.mdpi.com/journal/energies

Article

Electrodeposition of a Au-Dy_2O_3 Composite Solid Oxide Fuel Cell Catalyst from Eutectic Urea/Choline Chloride Ionic Liquid

Claudio Mele and Benedetto Bozzini *

Department of Innovation Engineering, University of Salento, via Monteroni, Lecce 73100, Italy; E-Mail: claudio.mele@unisalento.it

* Author to whom correspondence should be addressed; E-Mail: benedetto.bozzini@unisalento.it; Tel.: +39-0832-297-323; Fax: +39-0832-297-111.

Received: 15 August 2012; in revised form: 20 October 2012 / Accepted: 7 December 2012 / Published: 19 December 2012

Abstract: In this research we have fabricated and tested Au/Dy_2O_3 composites for applications as Solid Oxide Fuel Cell (SOFC) electrocatalysts. The material was obtained by a process involving electrodeposition of a Au-Dy alloy from a urea/choline chloride ionic liquid electrolyte, followed by selective oxidation of Dy to Dy_2O_3 in air at high temperature. The electrochemical kinetics of the electrodeposition bath were studied by cyclic voltammetry, whence optimal electrodeposition conditions were identified. The heat-treated material was characterised from the morphological (scanning electron microscopy), compositional (X-ray fluorescence spectroscopy) and structural (X-ray diffractometry) points of view. The electrocatalytic activity towards H_2 oxidation and O_2 reduction was tested at 650 °C by electrochemical impedance spectrometry. Our composite electrodes exhibit an anodic activity that compares favourably with the only literature result available at the time of this writing for Dy_2O_3 and an even better cathodic performance.

Keywords: Dy; Au; Dy_2O_3; electrodeposition; composite; solid oxide fuel cell (SOFC); urea; choline chloride; ionic liquid

1. Introduction

Solid oxide fuel cells (SOFCs) have received great attention in recent years as a viable high temperature fuel cell technology, because they offer the promise of high efficiency and fuel flexibility [1]. The most advanced SOFCs are those based on the so-called cermet anodes, which are

composed of Ni and an oxygen ion conducting ceramic such as yttria-stabilized zirconia (YSZ) or doped ceria (DCO) [2,3]. In these anodes, Ni acts as both the catalyst for electrochemical oxidation of the fuel and electronic conducting phase, while the ceramic possesses a substantial oxygen ionic conductivity, in order to increase the triple phase boundary region where anode, electrolyte and pores meet [4]. Recent studies have shown that Ni-LnO_x cermet anodes exhibit high electrochemical performance, comparable to the state-of-the-art anodes for intermediate temperature SOFCs, due to the high catalytic performance of lanthanide oxides [2,4,5]. In order to produce composite electrodes with different composition, some methods alternative to powder technologies have been proposed, as an approach based on the impregnation of soluble salts into the electrode layer and electrodeposition, a potentially simple method to incorporate the metallic component.

Among rare earth oxides, Dy_2O_3 has been demonstrated to have a good catalytic behaviour [4]. Dysprosium cannot be electrodeposited from aqueous solutions due to its negative electrode potential. Moreover dysprosium reacts very fast with the components of the atmosphere [6]. An alternative could be the use of non aqueous solutions and few studies have been conducted relating to the electrodeposition of dysprosium in ionic liquid [6–8]. The electrodeposition in ionic liquid is a specific way to obtain compounds of reactive and refractory elements as well as of actinides and rare earth metals [9,10] and presents some advantages in comparison with processes performed from aqueous solutions, among them: higher efficiency of electrolysis, lower energy consumption and much better characteristics of the deposits [9,11].

In previous research, we have developed methods for the co-electrodeposition of metal-ceramic composites [12–16]. In this work we have incorporated Dy_2O_3 into a Au matrix, fabricating Au-Dy_2O_3 composites by electrodeposition from a ionic liquid based on choline chloride and urea, followed by controlled oxidation. In this way an oxide with controlled nanometric structure, more suited for electrocatalytic work can be achieved. We used a gold matrix in order to devise a model system aiming at singling out the specific catalytic properties of finely dispersed dysprosium oxide, according to cognate SOFC literature discussing dispersed MnO_2 catalyst in a Au matrix [17,18]. Of course, it is relatively straightforward to replace Au with another metal that can be electrodeposited from the same solvent, such as Ni, if the target of the research is to fabricate a better performing catalyst for direct application. In the particular case of nickel, we have already demonstrated the feasibility of this process for the fabrication of Ni/ceria composites [16]. The present research represents the first step of a process aiming to achieve, by electrodeposition, the synthesis of nickel and rare earth oxides, having both good electronic and ionic conductivity [19–23], as potential materials for SOFC electrodes.

2. Results and Discussion

2.1. Electrodeposition of Au-Dy Alloy—Electrochemical Measurements

CVs of a GC electrode in 2:1 urea/ChCl ionic liquid without and with added $DyCl_3$ or $DyCl_3$ and $KAu(CN)_2$ are reported in Figure 1. The CV of the pure electrolyte [Figure 1 (A)] shows the extent of the double layer charging region, ranging from *ca.* 1.1 to *ca.* −1.75 V, where anodic and cathodic decomposition reactions of the ionic liquid occur. In the presence of $DyCl_3$ [Figure 1 (B)] we observed a current density increase at about −1.4 V, followed by a mass-transport controlled plateau, that can be

straightforwardly attributed to Dy electrodeposition [6,9], followed by a typical mass-transport controlled voltammetric peak, and by a further current density increase, due to the cathodic reactivity of the ionic liquid. In the presence of $KAu(CN)_2$ [Figure 1 (C)], a cathodic peak—corresponding to Au electrodeposition, followed by a diffusion-controlled plateau can be observed at *ca.* −0.3 V, decreasing to current density values that are much lower than those observed in the absence of the Au(I) salt. Since reagent consumption does not justify this low current density, it could be explained with cathodic passivation by adsorbed CN^- [24,25]. Coherently with the cathodic passivation found after the Au deposition process, the deposition potential for Dy is shifted cathodically with respect to the case of the pure-Dy bath. This passivation process, giving rise to higher crystallisation overvoltages, ensures the formation of nanocrystalline Dy in the Au matrix (see XRD results in Section 2.2) giving rise to optimal catalyst properties. The positive current density increase at potentials more anodic than *ca.* 0 V corresponds to Au oxidation [24–26]. From these voltammetric data, the potential of −1.8 V has been chosen for Au-Dy alloy electrodeposition: in correspondence of this potential in fact both Dy and Au might be deposited and this condition not yet leads to reduction of the ionic liquid. Thus, we performed potentiostatic electrodeposition experiments of growth of Au-Dy at the potential of −1.8 V for 2 hours.

Figure 1. Cyclic voltammetries (scan rate: 100 $mV \cdot s^{-1}$) for a glassy carbon electrode in: (**A**) 2:1 urea/ChCl; (**B**) 2:1 urea/ChCl with $DyCl_3$ 250 mM; (**C**) 2:1 urea/ChCl with $DyCl_3$ 250 mM and $KAu(CN)_2$ 10 mM.

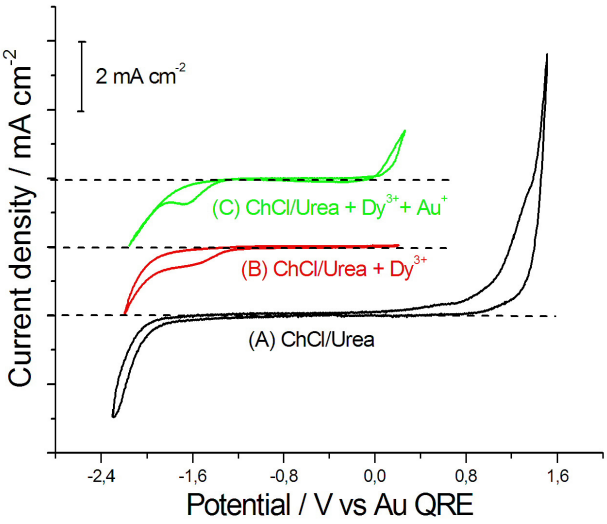

2.2. Morphology, Composition and Structure of Au-Dy Electrochemically Grown Films.

In Figure 2 we report SEM micrographs obtained at different magnifications of the Au-Dy alloy electrodeposited at the potential of −1.8 V for 2 hours, before Figure 2 (a) and after (b, c and d) heat treatment of 1 hour at 650 °C. The oxidised deposit presents a combination of morphological characteristics of electroplated metal ceramic stress-relief cracking. A granular and cracked morphology is desirable when a catalyst is used with a reactant gas, as in the case of a SOFC, whose porous electrodes are typically manufactured with powder metallurgy techniques. The EDX compositional analysis showed that dendrites represent zones rich in Au (3 wt.% of Dy), while the

background on which these dendrites are grown is rich in Dy (80 wt.% of Dy) (Figure 2 C), following the local current-density distribution and attending Mullins-Sekerka type growth instabilities [27]. The Dy-rich background gives rise to matrix cracking and the Au-rich dendrites exhibit a nanometric dispersion of Dy_2O_3.

Figure 2. SEM micrographs of Au-Dy electrochemically grown film at the potential of −1.8 V for 2 hour, before (**a**) and after (**b**, **c** and **d**) heat treatment at 650 °C for 1 hour.

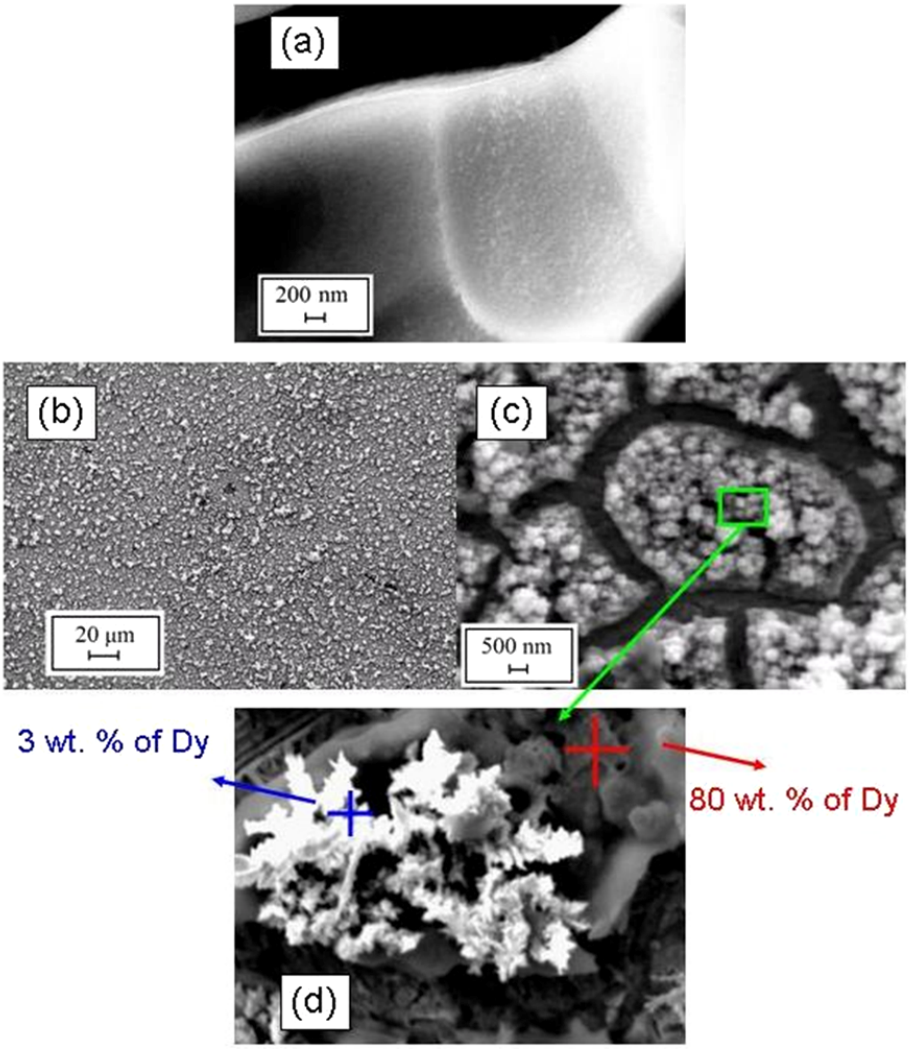

The structural characterization of the oxidized Au-Dy_2O_3 alloys has been carried out by X-ray diffractometry (Figure 3) [28]. Well-defined diffraction peaks of the Dy_2O_3 phase appear (JCPDS files #22-0612 and #04-0784), in addition to Au reflections. Scherrer analysis of the Dy_2O_3 peaks yields a characteristic grain dimension of *ca.* 13 nm.

Figure 3. X-ray diffractogram of Au-Dy_2O_3 alloy electrodeposited at the potential of −1.8 V for 2 hour, after heat treatment at 650 °C for 1 hour.

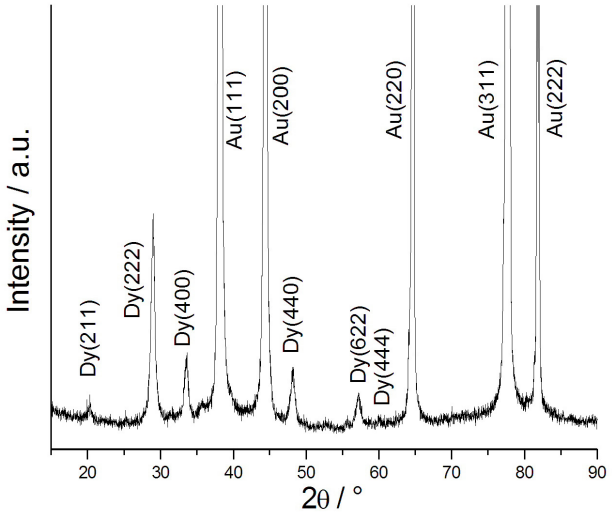

2.3. Single Cell Testing—Electrochemical Impedance Spectrometry

The electrocatalytic activity of the electrodeposited composite material was tested by electrochemical impedance spectrometry (EIS) under single-cell SOFC conditions at 650 °C in the system illustrated in Figure 4. Both the anodic and cathodic behaviour was considered, feeding the cell with hydrogen and with air, respectively. The interfacial polarization resistance R_p of the bare gold electrode used as anode resulted 4,220 Ω·cm^2 while that of Au-Dy_2O_3 composite was 1650 Ω cm^2 [Figure 5(a)], revealing a higher anodic catalytic activity of the Au-Dy_2O_3 composite compared with bare Au and confirming the only available literature result on this material [4]. This catalytic behaviour might be explained by an high H_2 consumption creating new active sites through hydrogen or oxygen spillover [4,29]. Even more evident effect was noticed by evaluating the catalytic activity of the novel material cathodic catalyst. In fact we found R_p values of 11,210 Ω·cm^2 for bare Au and 157 Ω·cm^2 for Au-Dy_2O_3 respectively [Figure 5(b)].

Figure 4. Schematic diagram of measurement apparatus employed for EIS experiments.

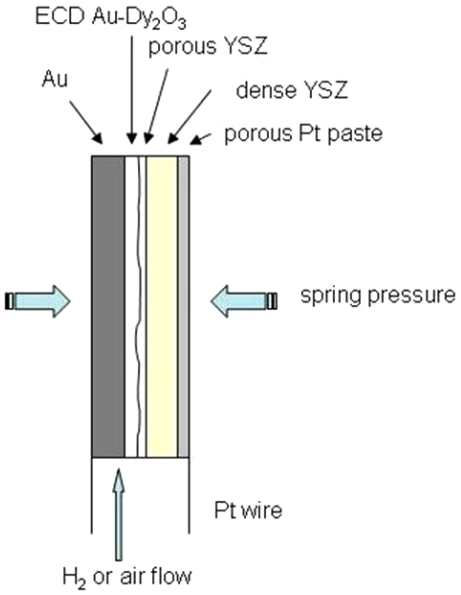

Figure 5. EIS spectra of the composite Au-Dy_2O_3 electrode as anode, feeding the single cell with hydrogen (**a**) or as cathode, feeding the cell with ambient air (**b**), measured at of 650 °C and applied bias potential of 1 V.

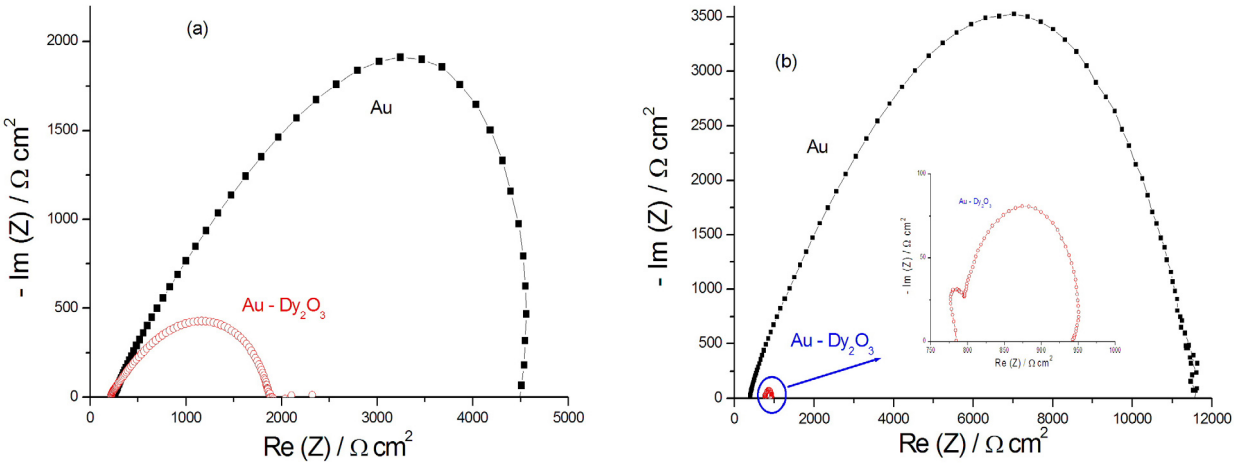

(a) **(b)**

3. Experimental Section

The ionic liquid formulation was prepared by mixing urea and choline chloride (ChCl) in a 2:1 molar ratio and heating at a temperature of 80 °C, with continuous magnetic stirring, until a clear colourless liquid was formed. Two electrodeposition solutions were obtained from the ionic liquid, by adding either $DyCl_3$ 250 mM or this same amount of Dy(III) with $KAu(CN)_2$ 10 mM: stirring for additional 30 min yielded a clear liquid. Cyclic voltammetry (CV) measurements at 100 mV s^{-1} were performed in order to characterise the pure electrolyte and the bath containing Dy with or without Au. A dysprosium-gold thin film was cathodically deposited at 80 °C under a nitrogen atmosphere in a glove box, in which the moisture and oxygen contents were maintained below 1 ppm. The deposited film was thoroughly cleaned with acetone and isopropanol, according to [30] and then it was oxidized in air at 650 °C for 1 hour.

Electrochemical measurement [potentiostatic deposition, cyclic voltammetry (CV) and electrochemical impedance spectrometry (EIS)] were carried out with an AMEL 5000 potentiostat/galvanostat connected to a frequency response analyzer (Solartron SI 1250). A three-electrode electrochemical cell was employed. The surface morphology and chemical composition of the electrodeposit were examined with a Cambridge Stereoscan scanning electron microscope (SEM) equipped with X-ray energy dispersive spectrometer (EDS). A Ultima+Rigaku diffractometer with a Bragg–Brentano goniometer was employed for XRD. For CV experiments and for compositional, structural and morphological studies the working electrode (WE) were, respectively, a glassy carbon (GC) rod of diameter 2 mm, embedded in Teflon and a polycrystalline Au disc of diameter 8 mm, respectively. The counter electrode (CE) was a graphite rod with an exposed area of 3 cm^2. A Au wire was chosen as the quasi-reference electrode (QRE), as customary in the literature and successfully tested in our own laboratory [18,31].

In order to estimate the electro-catalytic activity of the electrodeposited material, the apparatus described in Figure 4 was employed. A Au polycrystalline disc was used as the catalyst support, onto which the catalyst sample was electrodeposited and oxidised, as described above. A sheet of

yttria-stabilised zirconia (YSZ) with thickness 0.5 mm (Goodfellow ZR613051) was used as electrolyte. Porous tapes of YSZ, were prepared by tape casting with graphite pore formers using aqueous-based slurries of YSZ (Tosoh, 8 mol% Y_2O_3), followed by sintering at 1550 °C as described in [32] and were painted onto one side of the dense YSZ electrolyte. The electrolyte, composed of a compact YSZ support, coated with a porous YSZ layer, was pressed against the electroplated samples by using the spring load of the sample-holder depicted in Figure 4. A thin layer of porous platinum paste—acting as counter electrode and the gas distribution layer—was applied on the back-side of YSZ electrolyte and contacted via Pt wire. The cell was then sealed in a quartz cylinder and inserted in an oven at 650 °C. H_2 was used as the fuel to test the samples as anode and ambient air to test them as cathodes: in both cases we used a flow rate of 30 $mL \cdot min^{-1}$. Electrochemical impedance experiments were performed in the frequency range from 0.01 to 100 kHz, with a sinusoidal potential modulation of 0.1 V peak-to-peak and a bias of +1 and −1 V for anodic and cathodic tests, respectively.

4. Conclusions

In this paper, we report on the successful electrodeposition of dysprosium and its alloy with metals of very different nobility (Au-Dy) from an eutectic choline chloride/urea ionic liquid. In this way, with a single electrodeposition process, followed by heat treatment, we obtained a composite Au-Dy_2O_3 usable as SOFC electrode. In fact, test of our composite material as SOFC electrode demonstrated good electrocatalytic cathodic and anodic behaviour. The anodic behaviour observed in the literature for a cermet manufactured from powders was confirmed by our electrochemically grown material and the obtained composite demonstrated even better behaviour as cathode, not yet reported in the literature.

References

1. McIntosh, S.S.; Gorte, R.J. Direct hydrocarbon solid oxide fuel cells. *Chem. Rev.* **2004**, *104*, 4845–4865.
2. He, B.B.; Ding, D.; Xia, C.R. Ni–LnO_x (Ln = La, Ce, Pr, Nd, Sm, Eu, and Gd) cermet anodes for intermediate-temperature solid oxide fuel cells. *J. Power Sources* **2010**, *195*, 1359–1364.
3. De Boer, B.; Gonzalez, M.; Bouwmeester, H.J.M.; Verweij, H. The effect of the presence of fine YSZ particles on the performance of porous nickel electrodes. *Solid State Ionics* **2000**, *127*, 269–276.
4. He, B.; Zhao, L.; Wang, W.; Chen, F.; Xia, C. Electro-catalytic activity of Dy_2O_3 as a solid oxide fuel cell anode material. *Electrochem. Comm.* **2011**, *13*, 194–196.
5. Ding, D.; Li, L.; Feng, K.; Liu, Z.B.; Xia, C.R. High performance Ni–Sm_2O_3 cermet anodes for intermediate-temperature solid oxide fuel cells. *J. Power Sources* **2009**, *187*, 400–402.
6. Lodermeyer, J.; Multerer, M.; Zistler, M.; Jordan, S.; Gores, H.J.; Kipferl, W.; Diaconu, E.; Sperl, M.; Bayreuther, G. Electroplating of dysprosium, electrochemical investigations, and study of magnetic properties. *J. Electrochem. Soc.* **2006**, ***153***, 242–248.
7. Hsu, H.Y.; Yang, C.C. Conductivity, electrodeposition and magnetic property of Cobalt(II) and dysprosium chloride in Zinc Chloride-1-Ethyl-3-Methylimidazolium chloride room temperature molten salt. *Z. Naturforsch. B* **2003**, *58*, 139–146.

8. Kumbhar, P.P.; Lokhande, C.D. Electrodeposition of Dysprosium from nonaqueous Bath. *Indian J. Chem. Technol.* **1994**, *1*, 194–196.
9. Castrillejo, Y.; Bermejo, M.R.; Barrado, A.I.; Pardo, R.; Barrado, E.; Martínez, A.M. Electrochemical behaviour of Dysprosium in the eutectic LiCl–KCl at W and Al electrodes. *Electrochim. Acta.* **2005**, *50*, 2047–2057.
10. Taxil, P.; Chamelot, P.; Massot, L.; Hamel, C. Electrodeposition of alloys or compounds in molten salts and applications. *J. Min. Metall.* **2003**, *39*, 177–200.
11. Sheti, R.S. Electrocoating from molten salts. *J. Appl. Electrochem.* **1979**, *9*, 411–426.
12. Tondo, E.; Boniardi, M.; Cannoletta, D.; De Riccardis, M.F.; Bozzini, B.; Electrodeposition of Yttria/Cobalt-oxide and Yttria/Gold coatings onto ferritic stainless steel for SOFC interconnects. *J. Power Sources* **2010**, *195*, 4772–4778.
13. Bozzini, B.; Tondo, E.; Raffa, P.; Boniardi, M.; Electrodeposition of Y_2O_3-Au composite coatings for SOFC interconnects: *in situ* monitoring of film growth by surface-enhanced Raman spectroscopy. *Trans. Inst. Met. Fin.* **2012**, *90*, 30–37.
14. Hassannejad, H.; Mele, C.; Shahrabi, T.; Bozzini, B. Electrodeposition of Ni/ceria composites: an *in situ* visible reflectance investigation. *J. Solid State Electrochem.* **2012**, 16, 3429–3441.
15. Ding, B.Y.; Kim, Y.J.; Erlebacher, J. Nanoporous Gold Leaf: "Ancient Technology"/Advanced Material. *Adv. Mater.* **2004**, *16*, 1897–1900.
16. Mele, C.; Catalano, M.; Taurino, A.; Bozzini, B. Electrochemical fabrication of nanoporous gold-supported manganese oxide nanowires based on electrodeposition from eutectic urea/choline chloride ionic liquid. *Electrochim. Acta* **2013**, *87*, 918–924.
17. Kuhn, M.; Napporn, T.W. Single-chamber solid oxide fuel cell technology—from its origins to today's state of the art. *Energies* **2010**, *3*, 57–134.
18. Hibino, T.; Kuwahara, Y.; Wang, S. Effect of electrode and electrolyte modification on the performance of one-chamber solid oxide fuel cell. *J. Electrochem. Soc.* **1999**, *146*, 2821–2826.
19. Shuk, P.; Greenblatt, M.; Croft, M.; Hydrothermal synthesis and properties of mixed conducting $Ce_{1-x}Tb_xO_2$-deltasolid solutions. *Chem. Mater.* **1999**, *11*, 473–479.
20. Trovarelli, A. Catalytic properties of Ceria and CeO_2-Containing materials, *Catal. Rev. Sci. Eng.* **1996**, *38*, 439–520.
21. Fu, Q.; Saltsburg, H.; Flytzani-Stephanopoulous, M. Active nonmetaltic Au and Pt species on Ceria-based water-gas shift catalysts. *Science* **2003**, *301*, 935–938.
22. Fernández-García, M.; Martínez-Arias, A.; Guerrero-Ruiz, A.; Conesa, J.C.; Soria, J. Ce-Zr-Ca ternary mixed oxides: structural characteristics and oxygen handling properties. *J. Catal.* **2002**, *211*, 326–334.
23. Vlaic, G.; Di Monte, R.; Fornasiero, P.; Fonda, E.; Kašpar, J.; Graziani, M. Redox property-local structure relationships in the ph-loaded CeO_2-ZrO_2 mixed oxides. *J. Catal.* **1999**, *182*, 378–389.
24. Bozzini, B.; Tondo, E.; Bund, A.; Ispas, A.; Mele, C. Electrodeposition of Au from [EMIm][TFSA] room temperature ionic liquid: an electrochemical and Surface-Enhanced Raman Spectroscopy study. *J. Electroanal. Chem.* **2011**, *651*, 1–11.
25. Bozzini, B.; Busson, B.; Humbert, C.; Mele, C.; Raffa, P.; Tadjeddine, A. *In situ* SFG Investigation of Au electrodeposition from [BMP][TFSA], containing $KAu(CN)_2$. *J. Electroanal. Chem.* **2011**, *661*, 20–24.

26. Oyama, T.; Okajima, T.; Ohsaka, T. Electrodeposition of gold at glassy carbon electrodes in room-temperature ionic liquids. *J. Electrochem. Soc.* **2007**, *154*, 322–327.
27. Bozzini, B.; Lacitignola, D.; Mele, C.; Sgura, I. Coupling of morphology and chemistry leads to morphogenesis in electrochemical metal growth: a review of the reaction-diffusion approach. *Acta Appl. Math.* **2012**, *122*, 53–68.
28. Tok, H.A.I.Y.; Boey, F.Y.C.; Huebner, R.; Ng, S.H. Synthesis of dysprosium oxide by homogeneous precipitation. *J. Electroceram.* **2006**, *17*, 75–78.
29. Kili, K.; Hilaire, L.; Le Normand, F. Modification by lanthanide (La, Ce) promotion of catalytic properties of palladium: characterization of the catalysts. *Phys. Chem. Chem. Phys.* **1999**, *1*, 1623–1631.
30. Zein El Abedin, S.; Endres, F. Electrodeposition of nanocrystalline silver films and nanowires from the ionic liquid 1-ethyl-3-methylimidazolium trifluoromethylsulfonate. *Electrochim. Acta* **2009**, *54*, 5673–5677.
31. Bozzini, B.; Gianoncelli, A.; Kaulich, B.; Mele, C.; Prasciolu, M.; Kiskinova, M. Electrodeposition of manganese oxide from eutectic urea/choline chloride ionic liquid: an *in situ* study based on soft X-ray spectromicroscopy and visible reflectivity. *J. Power Sources* **2012**, *211*, 71–76.
32. Park, S.; Gorte, R.J.; Vohs, J.M. Tape cast solid oxide fuel cells for the direct oxidation of hydrocarbons. *J. Electrochem. Soc.* **2001**, *148*, 443–447.